

# Exploration of the Psychophysics of a Motion Displacement Hyperacuity Stimulus

Gay Mary Verdon-Roe,<sup>1,2</sup> Mark C. Westcott,<sup>3</sup> Ananth C. Viswanathan,<sup>1,2</sup> Frederick W. Fitzke,<sup>1</sup> and David F. Garway-Heath<sup>1,2</sup>

**PURPOSE.** To explore the summation properties of a motion-displacement hyperacuity stimulus with respect to stimulus area and luminance, with the goal of applying the results to the development of a motion-displacement test (MDT) for the detection of early glaucoma.

**METHODS.** A computer-generated line stimulus was presented with displacements randomized between 0 and 40 minutes of arc (min arc). Displacement thresholds (50% seen) were compared for stimuli of equal area but different edge length (orthogonal to the direction of motion) at four retinal locations. Also, MDT thresholds were recorded at five values of Michelson contrast (25%–84%) for each of five line lengths (11–128 min arc) at a single nasal location (−27,3). Frequency-of-seeing (FOS) curves were generated and displacement thresholds and interquartile ranges (IQR, 25%–75% seen) determined by probit analysis.

**RESULTS.** Equivalent displacement thresholds were found for stimuli of equal area but half the edge length. Elevations of thresholds and IQR were demonstrated as line length and contrast were reduced. Equivalent displacement thresholds were also found for stimuli of equivalent energy (stimulus area  $\times$  [stimulus luminance – background luminance]), in accordance with Ricco's law. There was a linear relationship (slope −0.5) between log MDT threshold and log stimulus energy.

**CONCLUSIONS.** Stimulus area, rather than edge length, determined displacement thresholds within the experimental conditions tested. MDT thresholds are linearly related to the square root of the total energy of the stimulus. A new law, the threshold energy-displacement (TED) law, is proposed to apply to MDT summation properties, giving the relationship  $T = K\sqrt{E}$  where,  $T$  is the MDT threshold,  $K$  is the constant, and  $E$  is the stimulus energy. (*Invest Ophthalmol Vis Sci.* 2006;47:4847–4855) DOI:10.1167/iovs.05-1487

We are developing a new perimetric motion-displacement test (MDT) for the early diagnosis of glaucoma called the Moorfields MDT. The original MDT was presented as a single vertical-line stimulus and has been shown by several published

studies to offer greater sensitivity to detect early glaucoma than does standard automated perimetry (SAP).<sup>1–5</sup> The MDT task is to determine the smallest perceptible positional displacement. The displacements give rise to the sensation of motion. Each stimulus presentation passes through three displacement cycles at 5 Hz.<sup>6,7</sup> The MDT differs from frequency-doubling technology (FDT) in that FDT uses larger grating stimuli, which are modulated in contrast and presented at a higher frequency of reversals (25 Hz). The MDT has been shown to be more resistant to the effect of cataract than both SAP and FDT.<sup>8,9</sup>

A fundamental requisite for understanding the normal psychophysiological response to a stimulus is to select appropriate stimulus parameters to obtain good test sensitivity and specificity that will distinguish normal and diseased states. Specifically, in this study we investigated the spatial summation characteristics of the MDT stimulus.

We have previously demonstrated equivalent MDT thresholds for stimuli of equivalent line length, whether the stimulus comprises a single line or three shorter lines (independent of line separation up to 128 minutes arc [min arc]).<sup>10</sup> The present study extends our earlier work and specifically explores summation properties of MDT stimuli in relation to line edge length, stimulus area, luminance, and contrast.

Scobey and Johnson<sup>11,12</sup> investigated the effect of changing line length and luminance using a unidirectional stimulus. Elevation of the displacement threshold was found as line length and luminance were decreased, with an increase in threshold mean and SD with eccentricity. Similar findings were reported by MacVeigh et al.<sup>13</sup> for an oscillating stimulus of low temporal frequency (2 Hz) in the presence of stationary references. The Moorfields MDT stimulus differs from these examples in that it undergoes three oscillations per presentation, which results in lower displacement thresholds when compared with a single oscillatory displacement.<sup>6</sup> It is presented at 5 Hz in the absence of stationary references. Direct comparison of the methodologies is therefore difficult.

It has been suggested that vernier thresholds are determined by the stimulus edge length.<sup>14–20</sup> In this study, we tested the hypothesis that it is the MDT stimulus area, rather than the edge length, that determines the threshold response, by comparing MDT thresholds for constant stimulus area but changing line edge length.

Previous studies have been performed to investigate vernier acuity as a function of contrast or line length.<sup>11,12,21</sup> In the present study we took a novel approach and calculated displacement thresholds as a function of the stimulus energy (stimulus area  $\times$  luminance) to explore the application of Ricco's Law to MDT stimuli. Standard automated perimetry (SAP) measures differential light sensitivity (DLS) and, where the stimulus lies within Ricco's critical area, the product of the area and intensity of the stimulus at threshold is constant.<sup>22</sup> There are no publications establishing whether Ricco's Law is applicable to an MDT-like stimulus, responses to which historically have been assumed to be mediated by the magnocellular (M) pathway.<sup>23</sup>

From the <sup>1</sup>Department of Visual Science, Institute of Ophthalmology, London, United Kingdom; <sup>2</sup>Glaucoma Research Unit, Moorfields Eye Hospital, London, United Kingdom; <sup>3</sup>St. Bartholomew's Hospital, London, United Kingdom.

Supported by an unrestricted grant by Pfizer.

Submitted for publication November 21, 2005; revised April 18 and May 22, 2006; accepted September 5, 2006.

Disclosure: **G.M. Verdon-Roe**, Pfizer (F); **M.C. Westcott**, Pfizer (F); **A.C. Viswanathan**, Pfizer (F); **F. W. Fitzke**, Pfizer (F); **D.F. Garway-Heath**, Carl Zeiss Meditec and Pfizer (F)

The publication costs of this article were defrayed in part by page charge payment. This article must therefore be marked "advertisement" in accordance with 18 U.S.C. §1734 solely to indicate this fact.

Corresponding author: Gay Mary Verdon-Roe, Glaucoma Research Unit, Moorfields Eye Hospital, London, UK; g.m.verdon-roe@ucl.ac.uk.

**TABLE 1.** The Seven Configuration Pairs for Stimuli of Equal Area and Various Line Lengths in Experiment 1

Field Location	Michelson Contrast (%)	Luminance (cd/m <sup>2</sup> )	Area (pixels)	Dimensions (pixels)	Aspect Ratio Width:Height
-27,3	85	112	96	12 × 8 24 × 4	1.5:1 6:1
-27,3	85	112	96	24 × 4 48 × 2	6:1 24:1
-27,3	55	34	64	16 × 4 32 × 2	4:1 16:1
-27,3	40	24	36	9 × 4 18 × 2	2.25:1 9:1
-9,15	55	34	24	6 × 4 12 × 2	1.5:1 6:1
-9,-15	55	34	64	16 × 4 32 × 2	4:1 16:1
3,9	25	17	24	6 × 4 12 × 2	1.5:1 6:1

## METHODS

The study design conformed to the tenets of the Declaration of Helsinki and had been passed by the local IRB. MDT testing was performed on a computer (Intel Pentium 4, 128 RAM; Windows ME) linked to a 21-in. monitor (1280 × 1024 pixels; 0.28 mm dot pitch; Hitachi, Tokyo, Japan). Luminances were estimated with a light meter (Chroma Meter CS-100; Minolta, Osaka, Japan) and the test background was maintained at 10 cd/m<sup>2</sup> (65 rgb [red-green-blue]) throughout the study. The field of uniformity of the monitor was estimated by measuring the 65 rgb and 255 rgb luminances, each three times, at 25 locations equally spaced in a 5 × 5 grid across the screen. The variation in Michelson contrast for these rgb values was ≤3%. Peripheral refractive error was estimated by retinoscopy in patients under mydriasis (tropicamide 1%). The subject fixated a central target, and the required corrective lenses were centered on a peripheral line stimulus, with an addition of +3.0 DSph to allow for the fixation distance of 30 cm. The line stimulus was programmed to pass through five presentations of each of seven randomized displacements (0–24 min arc). In each case, the vector of motion was orthogonal to the long edge of the line, which was aligned with the horizontal meridian. Each stimulus presentation consisted of three oscillations at 200 ms per cycle.<sup>7</sup> The subject task was to press the computer mouse each time a displacement was seen. Each test paradigm was applied in a randomized order and tested three times, so that each displacement was presented 15 times for each stimulus condition. The duration of each test was approximately 2 minutes 30 seconds. The number of tests was limited to eight per session, with rest intervals of 5 minutes between tests.

### Experiment 1: Variation of Stimulus Line Edge Length

The effect of halving the MDT stimulus line length, while maintaining equivalent area, was investigated for seven different configuration pairs of equal area.

Four retinal locations were tested using the specifications summarized in Table 1. Two subjects were tested for each configuration, with five perimetrically experienced subjects taking part in the investigation (age: mean 37 years, range 28–51).

### Experiment 2

Displacement thresholds were measured for five horizontal lines of length 4, 8, 16, 32, and 48 pixels (11, 22, 43, 86, and 128 min arc), each 2 pixels (5 min arc) wide, at each of five luminances (17, 24, 34, 56, and 112 cd/m<sup>2</sup>), equivalent to Michelson contrast of 25%, 40%, 55%, 70%, and 84%. In this experiment, the change in area equals the change

in line length. The line stimulus was positioned at a single location in the nasal field (-27,3, as indicated in Fig. 7) and programmed to pass through five presentations of each of seven randomized displacements (0, 1, 2, 3, 5, 7, and 9 pixels; equivalent to 0, 3, 5, 8, 14, 19, and 24 min arc). Additional tests were undertaken where no positive responses were made (all presentations unseen) to small lines of low contrast. When this occurred, the upper limit of displacement was increased to 40 min arc (five presentations of seven displacements: 0, 5, 7, 9, 11, 13, and 15 pixels; 0, 14, 19, 24, 30, 35, and 40 min arc). Two perimetrically experienced subjects were tested, aged 47 and 31 years.

## Data Analysis

**Experiments 1 and 2.** The results from the three test runs for each stimulus condition, for both experiments 1 and 2, were merged for each individual. Frequency of seeing (FOS) curves were generated, and the threshold was taken as the displacement corresponding to 50% seen of the probit fitted curve.

**Experiment 2: Additional Data Analysis.** The results of subjects 1 and 2 were averaged. The mean MDT threshold was plotted as a function of contrast for each line length on both linear and log coordinates. The interquartile range (IQR; difference between 75% and 25% of the probit fitted curve) was calculated to give an indication of the psychometric function slope.<sup>24,25</sup> The relation between mean log MDT threshold and log IQR was explored by linear regression analysis. Stimulus energy was calculated relative to background luminance as follows: relative stimulus energy = stimulus area × (stimulus luminance – background luminance). The background luminance was deducted from the stimulus luminance to account for the fact that, when the MDT stimulus is displaced, it moves to an area that is not black, but of constant background luminance (10 cd/m<sup>2</sup>). The relation between mean log MDT threshold and log relative stimulus energy was explored by linear regression analysis.

## RESULTS

### Experiment 1

The first experiment shows similar thresholds, with overlapping 95% confidence intervals (CIs), for stimulus configurations of equal area but different line edge length (Fig. 1).

### Experiment 2

The FOS curves of each subject illustrate a similar pattern of shallowing of the slope and widening of the 95% CI and IQR,

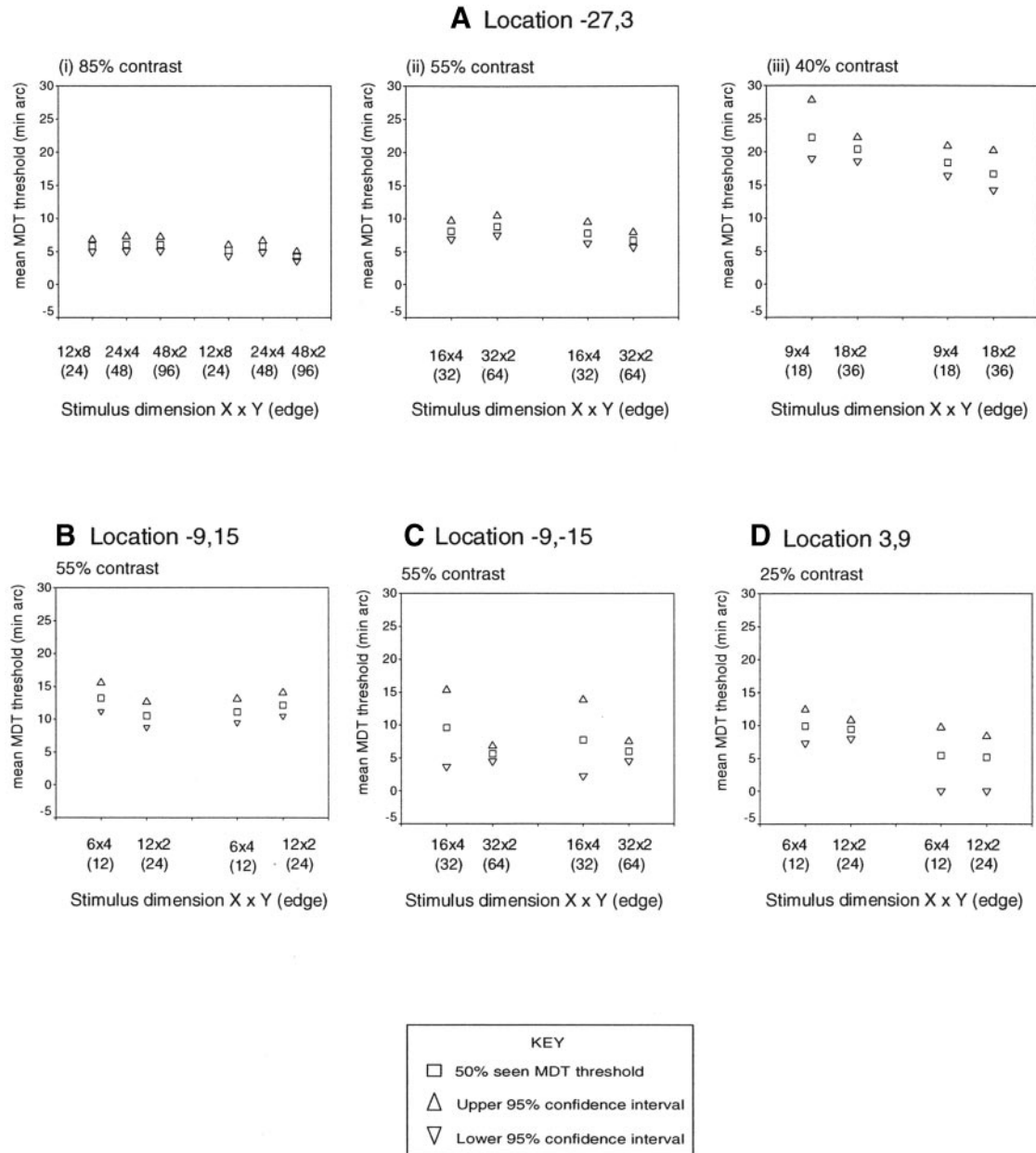


**FIGURE 1.** The effect of halving line length on MDT thresholds, while maintaining equivalent area. Locations: (A) -27,3; (B) -9, 15; (C) -9,-15; and (D) 3,9.

as contrast and line length is reduced, as shown by the selected examples (Fig. 2). Note the steep curve of the longest line length (128 min arc) at the highest contrast (85%), with a low IQR and narrow confidence intervals (Fig. 2A). Differences in psychometric function slopes remained when plotted on a logarithmic scale.

No responses were recorded for the smallest range of displacements (0 -24 min arc) when testing the smaller line lengths at low contrast (subjects 1 and 2: 11, 22, and 43 min arc line lengths at 25% contrast and the 11 min arc line length at 40% contrast; and subject 1: 22 min arc line length at 40% contrast). The increase in the upper limit of displacement to 40 min arc enabled only one further FOS curve to be measured for each subject (subject 1: 22 min arc line length

at 40% contrast; subject 2: 43 min arc line length at 25% contrast).

Analysis of MDT threshold as a function of contrast showed a curvilinear relationship for each line length, with an increase in threshold and widening of 95% CI, as contrast was reduced (Fig. 3). This relationship became linear when plotted in log-log coordinates (Fig. 4; Table 2). There was a linear relationship (slope: 1.3) between log MDT threshold and log IQR (Fig. 5). Log MDT thresholds were also linearly related to log relative stimulus energy, with a slope of approximately -0.5, indicating that the MDT threshold is related to the square root of the stimulus energy (Fig. 6). The slope for each subject was subject 1, -0.46 (95% CI -0.51 to -0.41;  $R^2 = 0.94, P < 0.001$ ) and subject 2, -0.43 (95% CI -0.36 to -0.49;  $R^2 = 0.88, P < 0.001$ ).

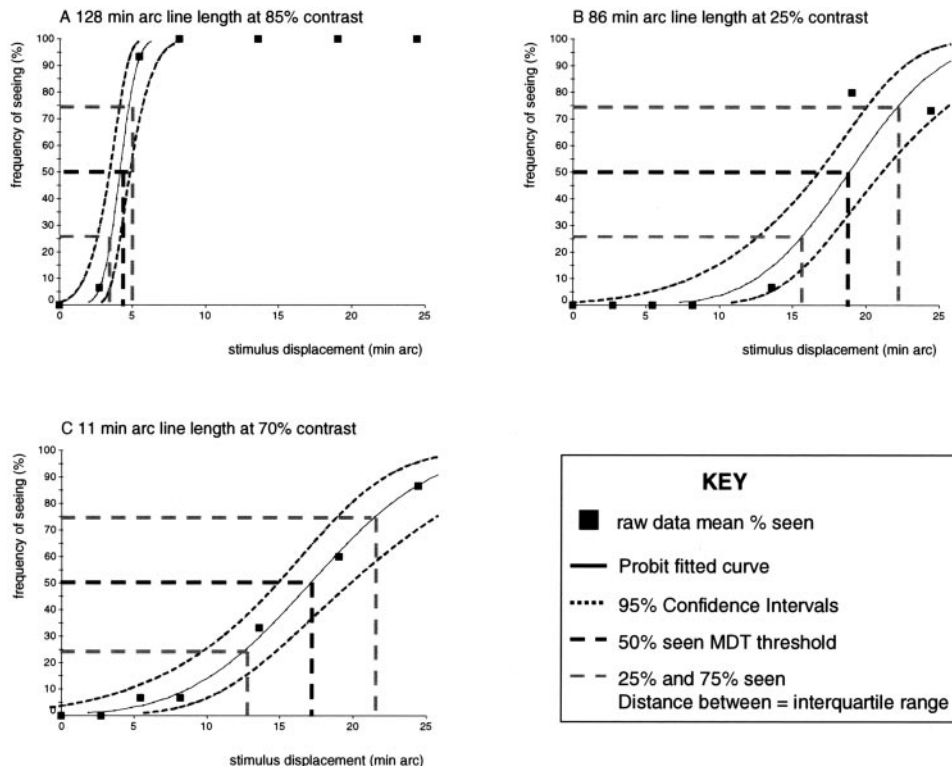


FIGURE 2. Examples of MDT FOS curves for individual subjects at varying line length and contrast: (A) 128 min arc (85% contrast); (B) 86 min arc (25% contrast); (C) 11 min arc (70% contrast).

## DISCUSSION

The MDT creates the illusion of motion by spatial displacement of a line stimulus. It is regarded as “local motion” which assumes the sampling of the image at two points in space at slightly different times by “bilocal” detectors.<sup>26</sup> Motion displacement has long been recognized as a hyperacuity stimulus, offering a sensitivity that is beyond that which would be predicted from anatomic ganglion cell spacing.<sup>27,28</sup> The MDT task is to discriminate positional change and may thus be categorized as a temporal form of vernier acuity.

Displacement acuity is conventionally considered to be a function of edge jump, with summation calculations being made in relation to line edge length.<sup>14,19</sup> The results of the first experiment (Fig. 1) suggest that it is the total area of the stimulus, as opposed to its edge length, that is the determining factor (for the range of parameters tested in the experiment). The wide CIs for the shorter but wider stimulus at retinal location  $-9, -15$  (Fig. 1C) may be explained by the stimulus' movement across a blood vessel (Fig. 7).

The second experiment shows a clear trend of decreasing MDT threshold with increasing line length and luminance (Fig. 3), which is consistent with previously reported findings of summation experiments for line displacement stimuli.<sup>12,13</sup> A re-analysis of 14 studies, which examined the relationship between contrast and vernier threshold as a power function, found log-log slopes ranging between  $-0.4$  and  $-1.0$ .<sup>21</sup> In this study, we found slopes ranging between  $-0.8$  and  $-1.2$  (Table 2).

The IQR scales directly with the MDT threshold (Fig. 5), with a slope of 1.26 (95% CI 0.98 to 1.54) on log-log coordinates. As line length and contrast are reduced, there is a shallowing of the FOS slope with elevation of IQR (Fig. 2) which is of an appearance similar to that seen in glaucoma,<sup>25</sup> where retinal ganglion cell (RGC) function is impaired. The increased variability seen with reduction in sensitivity is similar

to that found by Henson when assessing SAP in normal and diseased eyes, and which he attributed to a difference in functional ganglion cell density.<sup>29</sup> An alternative explanation is that the precision of the central detector is directly related to its spatial tuning, with greater precision associated with higher spatial frequency tuning.

There remains a widespread assumption that tests of motion are directed to the M pathway, although this may be an oversimplification. Clear segregation of the retinogeniculate pathways exists up to the lateral geniculate nucleus (LGN), but within the cortex multiple interconnections occur, making the pathways less independently driven than was once thought.<sup>30,31</sup>

The conventional view is that the M pathway acts as a motion-detection system which shows greater sensitivity, relative to the P pathway, to stimuli of low-contrast, high temporal frequency, and low spatial frequency.<sup>32-34</sup> The MDT conditions of this study are at a moderate temporal frequency (5 Hz), for stimuli of high spatial frequency, over a wide range of contrast (25%–85%). It is therefore possible that responses from both M and P contributions are invoked. However, this view is contradicted by a recent study, which suggests that the M pathway is primarily responsible for vernier acuity thresholds, with higher neural mechanisms being responsible for spatiotemporal integration.<sup>35</sup> Oscillatory displacement thresholds, measured in the presence of stationary references, have been shown to saturate at contrasts below 15%, consistent with the M pathway contrast response function.<sup>36</sup>

The energy plot (Fig. 6) shows a constant stimulus-response relationship over the range of contrasts assessed, which could apply to either a single or multiple pathway contribution. There is no evidence of a transitional shift in the threshold or slope, which would be a possible finding if different pathways were to predominate under different stimulus conditions within the experimental design. All stimuli were presented at

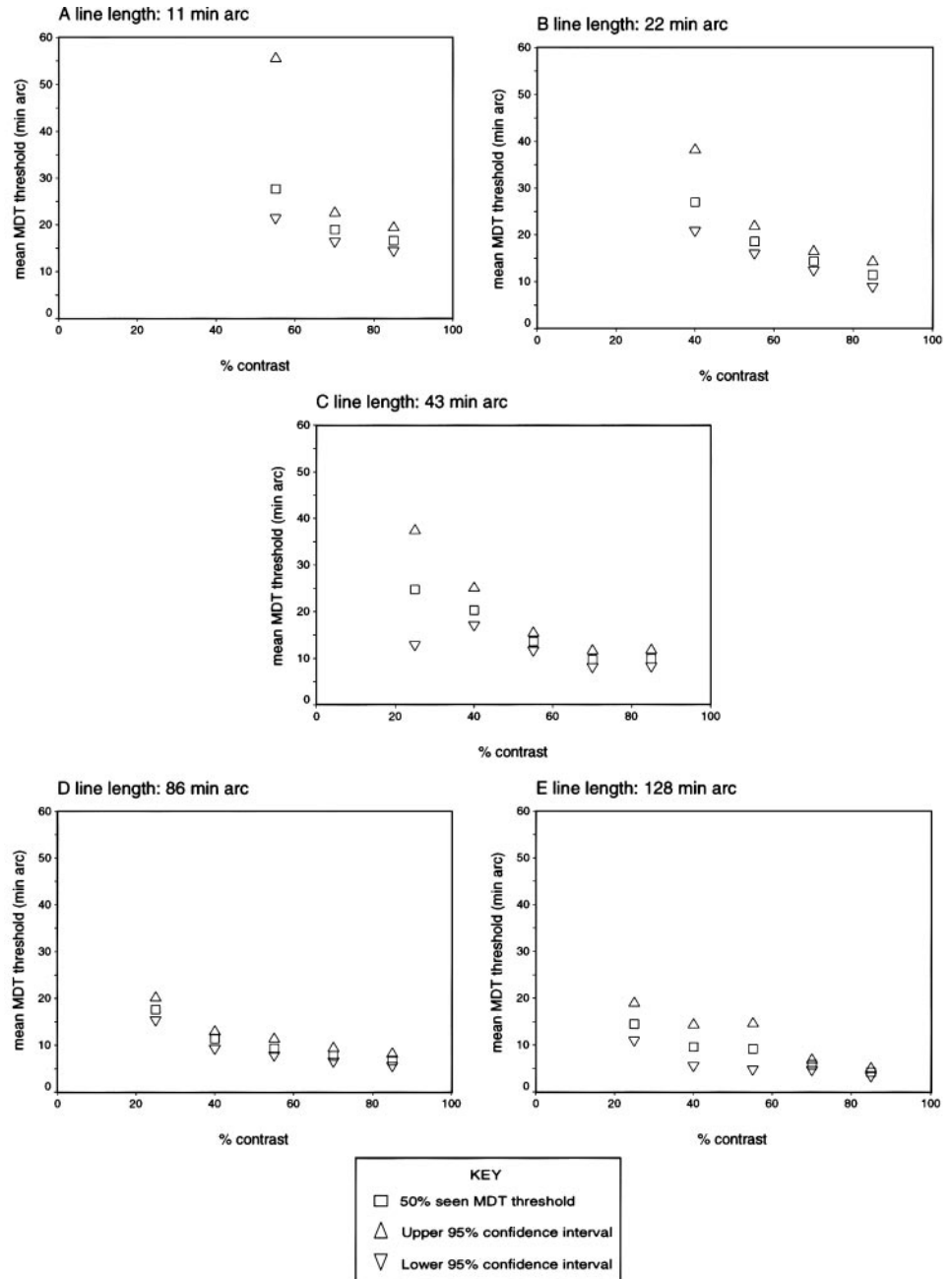


FIGURE 3. MDT threshold (average of two observers) versus contrast for each line length: (A) 11, (B) 22, (C) 43, (D) 86, and (E) 128 min arc.

contrasts equal to or greater than 25%, which is above the level at which the M pathway responses are generally considered to saturate. However, the results of this study suggest that it is not the contrast per se that modulates the response, but the stimulus energy (Fig. 6) so that saturation for higher contrast stimuli occurs only if the stimulus is also large. Saturation is generally measured with grating stimuli and so the “total energy” within a “receptive field” may be much larger than with the single-line displacement stimuli used in this experiment. It is therefore not possible to hypothesize mediation of the response by a particular cell type for these experimental conditions.

Table 3 shows the estimated number of RGCs stimulated by lines of various lengths. Values were approximated using estimates of human ganglion cell density (GCD)<sup>37</sup> and coverage values<sup>38</sup> (see the Appendix). The data in the table may under-

estimate the actual number of receptive fields stimulated, in that no allowance is given for the optical effect of line spread.<sup>39</sup>

All presentations at all displacements for the two shortest line lengths (11 and 22 min arc) were unseen, when testing at low contrast (25%–40%), even when the displacement range was increased to 40 min arc. The two smallest lines stimulate only a small number of ganglion cells (Table 3). It is possible that the energy these stimuli exert at low contrast is insufficient to generate a response. Alternatively, the displacement required at these energy levels may be greater than the detector receptive field.

The anatomic extent of the dendritic tree corresponds to the electrophysiological central receptive field, but may be smaller than the psychophysical receptive field estimate.<sup>43</sup> In humans, dendritic tree measurements approximate to 60-min

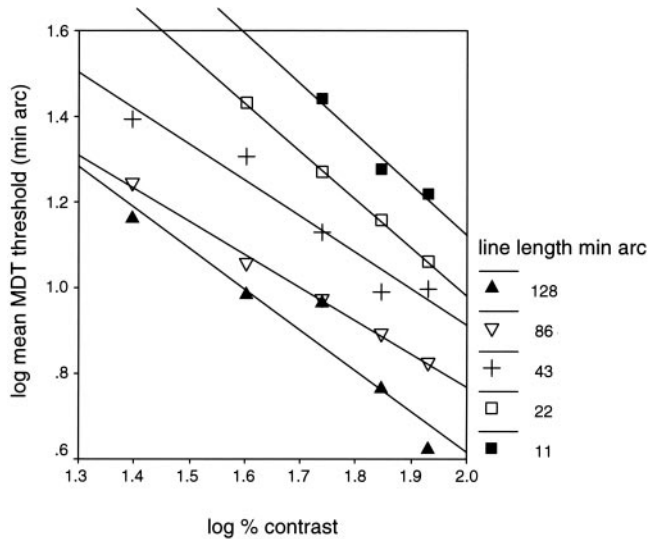


FIGURE 4. Relationship of the log mean MDT threshold (average of two observers) to log percentage contrast for each line length.

arc diameter for M cells and 20-min arc diameter for P cells, at 30° eccentricity in the nasal field (Fig. 8).<sup>38</sup> Human dendritic trees are larger than their counterparts in the macaque, predicting larger receptive fields.<sup>38</sup> The estimated psychophysical receptive field size in the macaque, at 30° eccentricity, for drifting sinusoidal gratings approximates 42 min arc.<sup>32,44,45</sup>

The slope of approximately  $-0.5$  of log MDT threshold against log stimulus energy (Fig. 6) is of special interest. To interpret this finding, the different processing mechanisms associated with SAP and MDT must be considered.

The threshold in SAP is determined by the relationship of the area (A) and intensity (I) of the stimulus, given by  $IA^n = \text{constant}$ . The summation coefficient ( $n$ ) varies for different conditions: Where the stimulus lies within Ricco's critical area,  $n = 1$ . ( $AI = \text{constant}$ ), and Ricco's law is said to hold. For larger stimuli, summation is incomplete, and the threshold is determined by probability summation, which is achieved by recruitment of adjacent receptive areas.<sup>46</sup> Piper's law holds when  $n = 0.5$ .<sup>22</sup>

The results of this study suggest that the same stimulus-threshold relationship may hold for the MDT stimulus. Longer lines extend over many ganglion cells, yet result in the same threshold as shorter, brighter lines of equivalent energy (area  $\times$  luminance; Fig. 6). This is consistent with linear summation of RGC responses for the line lengths used in these experiments. Ricco's law holds for the stimulus parameters tested in this study (Fig. 6), so that there is a constant MDT threshold where the product of line length and luminance is constant.

TABLE 2. Slope Values of Log Mean MDT as a Function of Log Contrast

Line Length (min arc)	Slope (95% CI)	R <sup>2</sup>	P
128	-0.95 (-1.28, -0.62)	0.92	0.011
86	-0.78 (-0.84, -0.71)	1.00	<0.001
43	-0.84 (-1.07, -0.61)	0.95	0.005
22	-1.12 (-1.16, -1.10)	1.00	<0.001
11	-1.18 (-1.69, -0.68)	0.96	0.136

See log contrast data in Figure 4.

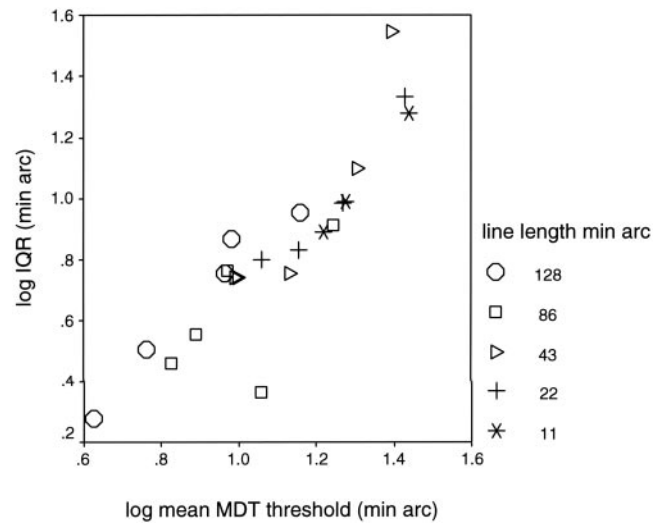


FIGURE 5. Log interquartile range as a function of log MDT threshold (average of two observers). Slope: 1.26 (95% CI, 0.98 to 1.54;  $R^2 = 0.79$ ;  $P < 0.001$ ).

Ricco's area is psychophysically defined<sup>22</sup> and estimates of the size of Ricco's critical area vary according to the type of the stimulus,<sup>47</sup> indicating different patterns of spatial filtering.<sup>44</sup> Ricco's area changes with eccentricity and this is thought to reflect changes in the underlying ganglion cell type, density, and neural convergence.<sup>47,48</sup> In humans, Ricco's area measures larger than the estimated anatomic dendritic field size, suggesting summation across RGCs and possible higher neural input.<sup>49</sup>

By contrast with DLS, electrophysiological studies of spot light displacement in primates indicate that all RGCs respond to movement of  $<10\%$  the diameter of their receptive field. It is thought that intrareceptive field directional sensitivity is achieved by pooling of the excitatory and inhibitory responses of overlapping on-off receptive fields.<sup>27,50</sup> The displacement threshold is thus determined by the sensitivity gradient between the two stimulus positions.<sup>12,51</sup> It is possible that, as the line stimulus oscillates from one position to another, different

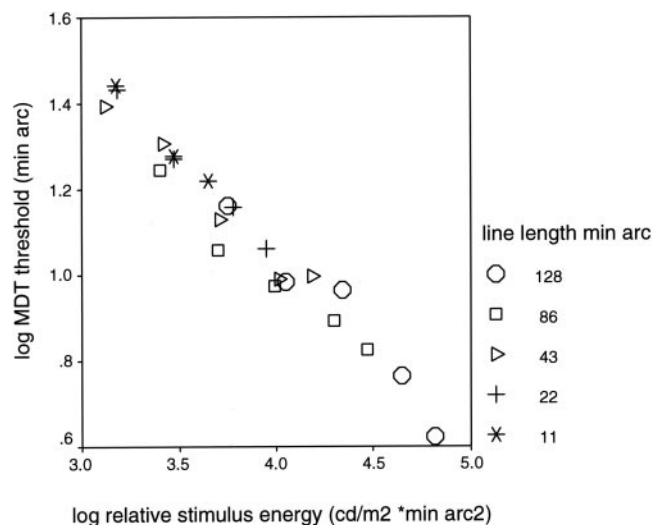
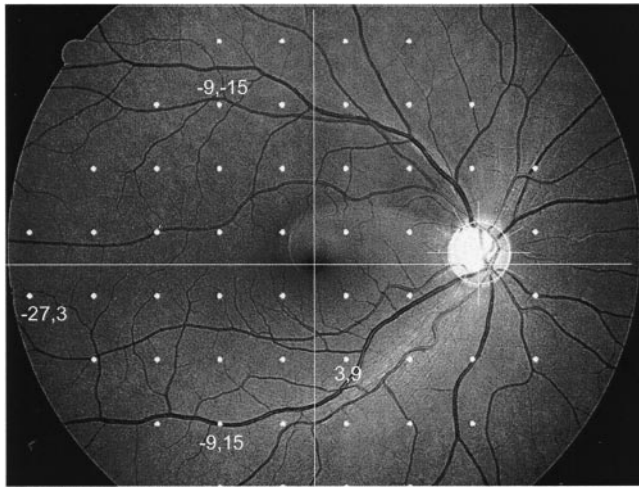


FIGURE 6. Log MDT (average of two observers) as a function of log stimulus energy: [energy = stimulus area  $\times$  (stimulus luminance - background luminance)]. Slope:  $-0.45$  (95% CI  $-0.49$  to  $-0.41$ ;  $R^2 = 0.96$ ;  $P < 0.001$ ).



**FIGURE 7.** Location of MDT locations on the retina. Note the proximity of blood vessels with locations 9,-15 and -9,-15. Retinal map reprinted from *Ophthalmology*, 107, Garway-Heath DF, Poinosawmy D, Fitzke FW, Hitchings RA, Mapping the visual field to the optic disc in normal tension glaucoma eyes, pages 1809-1815, Copyright 2000, with permission from the American Academy of Ophthalmology.

parts of the concentric on/off ganglion cell receptive fields are stimulated as an alternating decremental-incremental response.

A route to understanding the relationship between stimulus energy and the MDT threshold lies in ideal detector modeling, whereby a hypothetical model of optimal performance is created for known variables. Geisler<sup>52</sup> predicted a slope of 0.5 between log threshold and log stimulus intensity for a hyperacuity stimulus calculated on the basis of preneural factors (line-spread function, pupil size, retinal receptor anatomy, and Poisson distribution of photon absorption) and an ideal detector. This conclusion is consistent with the findings of the present study. The optimal receptive field was built by simple linear summation and inhibition. In a later paper, Geisler and Diehl<sup>53</sup> advise consideration of both preneural and hierarchical neural factors, with receptive fields regarded as free parameters.

The quantal absorption of photons by the retinal detectors is a source of noise described by the Poisson distribution. Noise is a constant feature in all sensory pathways, and signal detection is dependent on the average number of quantal absorptions necessary to elicit one extra impulse. This level determines gain control, and the signal-to-noise ratio grows in proportion to the square root of the stimulus area.<sup>54,55</sup>

Previous studies have suggested that vernier acuity is predicted from changes in the relative luminance of the retinal

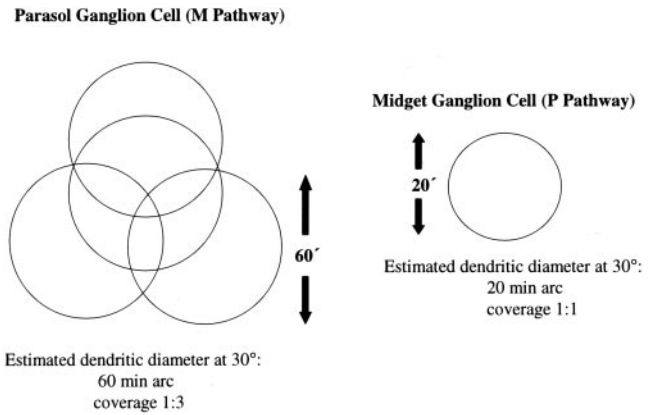


**FIGURE 8.** Anatomic estimate of human dendritic receptive field (RF) and coverage for M (Parasol) and P (Midget) cells at 30° eccentricity.<sup>38,40</sup>

image.<sup>56-58</sup> The results of the present study indicate that MDT sensitivity is achieved by detection of the total energy difference as the stimulus is displaced with respect to its environment. The MDT stimulus is displaced in position over time and is therefore probably best modeled using a three-dimensional space-space-time filter input.<sup>59</sup> Adelson and Bergen<sup>60</sup> suggested a two-stage hierarchical model of local motion signals, in which the first stage represents pairs of linear filters that are oriented in space and time and tuned in spatial frequency. The response of each pair is squared and summed. The second stage computes “motion energy” on the assumption of neural opponence. The MDT is an oscillating “A-B-A” square wave stimulus of apparent motion. The displacement threshold may therefore represent the summed difference of the on-off responses and also opposing directional filters, as the stimulus is displaced from position “A” to second position “B” and back to starting position “A.”

The novel finding of this study is that the MDT threshold is related to the square root of the stimulus energy for the stimulus conditions described. Thus, a new principle, TED (threshold energy displacement), is proposed to apply to MDT summation properties, giving the relationship:  $T = K \sqrt{E}$  (where  $T$  is the MDT threshold,  $K$  is the constant, and  $E$  is the stimulus energy: stimulus area  $\times$  stimulus luminance - background luminance). TED offers a numerical basis for modeling the structural-functional relationship of MDT thresholds and will be applied to the new multilocation MDT under development. It is anticipated that there is the potential to quantify neural losses from glaucoma with MDT using the principles described for SAP.<sup>44,61,62</sup> Future work will explore the relationship of MDT thresholds with stimulus energy at other retinal locations.

**TABLE 3.** Estimated Number of Retinal Ganglion Cells Stimulated by the MDT Stimulus, in the Nasal Field at 30° Eccentricity

Line Length (min arc)	Total RGCs	M “On” and “Off”	P “On” and “Off”	P “On”	P “Off”
128	18	12	8	3	5
86	12	9	5	2	3
43	6	6	3	1	2
22	3	3	2	<1	1
11	2	1	1	<1	<1

Data are the number of RGCs stimulated by target.<sup>37,38,40-42</sup> The methods of the calculations are given in the appendix. Each length was a uniform width of 2 pixels (5 min arc).

## Acknowledgments

The authors thank Bill Swanson and Hao Sun for helpful comments during the preparation of the manuscript and the fellows of the Glaucoma Research Unit at Moorfields who were subjects in the experiments.

## APPENDIX

### Calculation of Number of Ganglion Cells Stimulated by a Line Stimulus at $-27,3$

Line length (in millimeters) = degree subtended  $\times$  magnification factor.

$$\text{Eccentricity} = \sqrt{(x^2) + (y^2)}.$$

Therefore, eccentricity at  $x = 27$  and  $y = 3$  is  $\sqrt{(27 \times 27) + (3 \times 3)} = 27.16$ .

$$\text{Magnification} = 0.286 - [0.000014(\text{ecc}^2)].$$

Therefore, magnification at 27.16 is  $0.286 - [0.000014(27.16 \times 27.16)] = 0.276$ .

Number of ganglion cells stimulated = line length (in millimeters)  $\times$  linear estimate of ganglion cell numbers.

Estimated ganglion cell density at  $27.16^\circ = 877$  ganglion cells per  $\text{mm}^2$ .<sup>37,62</sup>

Linear estimate =  $\sqrt{\text{GCD}} = 30$  ganglion cells per millimeter.

### Example of Calculation of the Number of RGCs Stimulated at $27,3$ by a 128-min arc Length Line

Line length is 128 min arc =  $2.13^\circ = (0.276 \times 2.13)$  mm = 0.588 mm.

Line width is 5 min arc =  $0.08^\circ = 0.02208$  mm.

Therefore stimulus length stimulates  $0.588 \times 30 = 17.6 \sim 18$  ganglion cells (all types).

Width stimulates:  $0.022 \times 30 = 0.66$  ganglion cells (all types).

### Calculation of the Number of P and M Cells and Coverage Values for each "On" and "Off" Mosaic

The number of P (midget) and M (parasol) cells was estimated from percentage estimates of each cell type from primate histologic data. At  $30^\circ$  eccentricity, this approximated to 20% parasol and 45% midget.<sup>40</sup>

Coverage is defined as the average number of cells with receptive-field centers that include the same point in visual space. It is identical with overlap (the average number of cells with receptive fields that cover that of a given cell).<sup>63</sup> The anatomic estimate of coverage is given by cell density (in square millimeters)  $\times$  dendritic field area (in square millimeters).<sup>40</sup> The calculations are adjusted for coverage of each "on" and "off" mosaic.<sup>38,42</sup> The estimated coverage is 3:1 for the parasol cells and 1:1 for the midget cells.<sup>40</sup> Calculations are further adjusted for the higher cell density of "off" P cells, located in the outer inner plexiform layer (IPL), compared with "on" P cells, which are located in the inner IPL (outer: inner density ratio of 1.7:1).<sup>42</sup> M cells are assumed to be divided equally between "off" and "on" mosaics.

## References

1. Fitzke FW, Poinoosawmy D, Ernst W, Hitchings RA. Peripheral displacement thresholds in normals, ocular hypertensives and glaucoma. In: Greve E, Heijl A, eds. *Perimetry Update 1986/1987*. The Hague, The Netherlands: Kugler & Ghedini; 1987:447-452.
2. Fitzke FW, Poinoosawmy D, Nagasubramanian S, Hitchings RA. Peripheral displacement thresholds in glaucoma and ocular hypertension. In: Heijl A, ed. *Perimetry Update 1988/1989*. The Hague, The Netherlands: Kugler & Ghedini; 1989:399-405.
3. Ruben S, Fitzke F. Correlation of peripheral displacement thresholds and optic disc parameters in ocular hypertension. *Br J Ophthalmol*. 1994;78:291-294.
4. Baez KA, McNaught AI, Dowler JG, Poinoosawmy D, Fitzke FW, Hitchings RA. Motion detection threshold and field progression in normal tension glaucoma. *Br J Ophthalmol*. 1995;79:125-128.
5. Poinoosawmy D, Fitzke FW, Wu X, Hitchings RA. Discrimination between progression and non-progression visual field loss in low tension glaucoma using MDT. In: Mills RP, ed. *Perimetry Update 1992/1993*. Kugler Publications; 1992:109-114.
6. Verdon-Roe GM, Westcott MC, Viswanathan AC, Fitzke FW, Hitchings RA. Optimum number of stimulus oscillations for motion displacement detection in glaucoma. In: Wall M, Wild J, eds. *Perimetry Update 2000/2001*. The Hague, The Netherlands: Kugler Publications; 2000:97-102.
7. Westcott MC, Verdon-Roe GM, Viswanathan AC, Fitzke FW, Hitchings RA. Optimum stimulus duration for motion displacement detection in glaucoma. In: Wall M, Wild J, eds. *Perimetry Update 2000/2001*. The Hague, The Netherlands: Kugler Publications; 2000:103-108.
8. Membrey L, Fitzke FW. Effect of lens opacity on white-on-white perimetry, frequency doubling perimetry, and motion detection perimetry. In: Wall M, Wild J, eds. *Perimetry Update 2000/2001*. The Hague, The Netherlands: Kugler Publications; 2000:259-266.
9. Membrey L, Kogure S, Fitzke FW. A comparison of the effects of neutral density filters and diffusing filters on motion perimetry, white on white perimetry and frequency doubling perimetry. In: Wall M, Wild J, eds. *Perimetry Update 1998/1999*. Kugler Publications; The Hague, The Netherlands; 1998:75-83.
10. Verdon-Roe GM, Garway-Heath DF, Westcott MC, Viswanathan AC, Fitzke FW. Spatial summation for single line and multi-line motion stimuli. In: Wall M, Henson DB, eds. *Perimetry Update 2002/2003*. The Hague, The Netherlands: Kugler; 2002:335-340.
11. Scobey RP, Johnson CA. Psychophysical properties of displacement thresholds for moving targets. *Acta Psychol (Amst)*. 1981; 48:49-55.
12. Johnson CA, Scobey RP. Foveal and peripheral displacement thresholds as a function of stimulus luminance, line length and duration of movement. *Vision Res*. 1980;20:709-715.
13. MacVeigh D, Whitaker D, Elliott DB. Spatial summation determines the contrast response of displacement threshold hyperacuity. *Ophthalmic Physiol Opt*. 1991;11:76-80.
14. Foley-Fisher JA. The effect of target line length on Vernier acuity in white and blue light. *Vision Res*. 1973;13:1447-1454.
15. Fendick MG, Swindale NV. Vernier acuity for edges defined by flicker. *Vision Res*. 1994;34:2717-2726.
16. Mather G. The dependence of edge displacement thresholds on edge blur, contrast, and displacement distance. *Vision Res*. 1987; 27:1631-1637.
17. Lee BB, Wehrhahn C, Westheimer G, Kremers J. Macaque ganglion cell responses to stimuli that elicit hyperacuity in man: detection of small displacements. *J Neurosci*. 1993;13:1001-1009.
18. Ruttiger L, Lee BB. Chromatic and luminance contributions to a hyperacuity task. *Vision Res*. 2000;40:817-832.
19. Lee BB, Wehrhahn C, Westheimer G, Kremers J. The spatial precision of macaque ganglion cell responses in relation to vernier acuity of human observers. *Vision Res*. 1995;35:2743-2758.
20. Watt RJ, Morgan MJ. The recognition and representation of edge blur: evidence for spatial primitives in human vision. *Vision Res*. 1983;23:1465-1477.
21. McIlhagga W, Paakkonen A. Effects of contrast and length on vernier acuity explained with noisy templates. *Vision Res*. 2003; 43:707-716.
22. Glezer VD. The receptive fields of the retina. *Vision Res*. 1965;5: 497-525.
23. Livingstone MS, Hubel DH. Psychophysical evidence for separate channels for the perception of form, color, movement, and depth. *J Neurosci*. 1987;7:3416-3468.

24. Chauhan BC, Tompkins JD, LeBlanc RP, McCormick TA. Characteristics of frequency-of-seeing curves in normal subjects, patients with suspected glaucoma, and patients with glaucoma. *Invest Ophthalmol Vis Sci.* 1993;34:3534-3540.
25. Westcott MC, Fitzke FW, Crabb DP, Hitchings RA. Characteristics of frequency-of-seeing curves for a motion stimulus in glaucoma eyes, glaucoma suspect eyes, and normal eyes. *Vision Res.* 1999;39:631-639.
26. Snowden RJ, Braddick OJ. The combination of motion signals over time. *Vision Res.* 1989;29:1621-1630.
27. Scobey RP, Horowitz JM. Detection of image displacement by phasic cells in peripheral visual fields of the monkey. *Vision Res.* 1976;16:15-24.
28. Westheimer G. Visual acuity and hyperacuity (editorial). *Invest Ophthalmol.* 1975;14:570-572.
29. Henson DB, Chaudry S, Artes PH, Faragher EB, Ansons A. Response variability in the visual field: comparison of optic neuritis, glaucoma, ocular hypertension, and normal eyes. *Invest Ophthalmol Vis Sci.* 2000;41:417-421.
30. DeYoe EA, Felleman DJ, Van Essen DC, McClendon E. Multiple processing streams in occipitotemporal visual cortex. *Nature.* 1994;371:151-154.
31. Merigan WH, Maunsell JH. How parallel are the primate visual pathways? *Annu Rev Neurosci.* 1993;16:369-402.
32. Derrington AM, Lennie P. Spatial and temporal contrast sensitivities of neurones in lateral geniculate nucleus of macaque. *J Physiol.* 1984;357:219-240.
33. Merigan WH, Byrne CE, Maunsell JH. Does primate motion perception depend on the magnocellular pathway? *J Neurosci.* 1991;11:3422-3429.
34. Merigan WH, Katz LM, Maunsell JH. The effects of parvocellular lateral geniculate lesions on the acuity and contrast sensitivity of macaque monkeys. *J Neurosci.* 1991;11:994-1001.
35. Sun H, Ruttiger L, Lee BB. The spatiotemporal precision of ganglion cell signals: a comparison of physiological and psychophysical performance with moving gratings. *Vision Res.* 2004;44:19-33.
36. Watkins R, Buckingham T. The influence of stimulus luminance and contrast on hyperacuity thresholds for oscillatory movement. *Ophthalmic Physiol Opt.* Jan 1992;12:33-37.
37. Curcio CA, Allen KA. Topography of ganglion cells in human retina. *J Comp Neurol.* 1990;300:5-25.
38. Dacey DM, Petersen MR. Dendritic field size and morphology of midget and parasol ganglion cells of the human retina. *Proc Natl Acad Sci USA.* 1992;89:9666-9670.
39. Westheimer G. Visual acuity and hyperacuity: resolution, localization, form. *Am J Optom Physiol Opt.* 1987;64:567-574.
40. Dacey DM. Physiology, morphology and spatial densities of identified ganglion cell types in primate retina. *Ciba Found Symp.* 1994;184:12-28.
41. Dacey DM, Brace S. A coupled network for parasol but not midget ganglion cells in the primate retina. *Vis Neurosci.* 1992;9:279-290.
42. Dacey DM. The mosaic of midget ganglion cells in the human retina. *J Neurosci.* Dec 1993;13:5334-5355.
43. Croner LJ, Kaplan E. Receptive fields of P and M ganglion cells across the primate retina. *Vision Res.* Jan 1995;35:7-24.
44. Swanson WH, Feliuss J, Pan F. Perimetric defects and ganglion cell damage: interpreting linear relations using a two-stage neural model. *Invest Ophthalmol Vis Sci.* 2004;45:466-472.
45. Crook JM, Lange-Malecki B, Lee BB, Valberg A. Visual resolution of macaque retinal ganglion cells. *J Physiol.* 1988;396:205-224.
46. Robson JG, Graham N. Probability summation and regional variation in contrast sensitivity across the visual field. *Vision Res.* 1981;21:409-418.
47. Feliuss J, Swanson WH, Fellman RL, Lynn JR, Starita RJ. Spatial summation for selected ganglion cell mosaics in patients with glaucoma. In: Wall M, Heijl A, eds. *Perimetry Update 1996/1997.* The Hague, The Netherlands: Kugler Publications; 1996:213-221.
48. Volbrecht VJ, Shrago EE, Scheffrin BE, Werner JS. Spatial summation in human cone mechanisms from 0 degrees to 20 degrees in the superior retina. *J Opt Soc Am A Opt Image Sci Vis.* 2000;17:641-650.
49. Anderson RS. The psychophysics of glaucoma: improving the structure/function relationship. *Prog Retin Eye Res.* 2005;25:77-97.
50. Scobey RP. Movement sensitivity of retinal ganglion cells in monkey. *Vision Res.* 1981;21:181-190.
51. Zhang Y, Reid RC. Single-neuron responses and neuronal decisions in a vernier task. *Proc Natl Acad Sci USA.* 2005;102:3507-3512.
52. Geisler WS. Physical limits of acuity and hyperacuity. *J Opt Soc Am A.* 1984;1:775-782.
53. Geisler WS, Diehl RL. Bayesian natural selection and the evolution of perceptual systems. *Philos Trans R Soc Lond B Biol Sci.* 29 2002;357:419-448.
54. Rose A. The sensitivity performance of the human eye on an absolute scale. *J Opt Soc Am.* 1948;38:196-200.
55. Barlow HB, Levick WR. Three factors limiting the reliable detection of light by retinal ganglion cells of the cat. *J Physiol.* 1969;200:1-24.
56. Morgan MJ, Aiba TS. Vernier acuity predicted from changes in the light distribution of the retinal image. *Spat Vis.* 1985;1:151-161.
57. Westheimer G, McKee SP. Integration regions for visual hyperacuity. *Vision Res.* 1977;17:89-93.
58. Levi DM, McGraw PV, Klein SA. Vernier and contrast discrimination in central and peripheral vision. *Vision Res.* 2000;40:973-988.
59. Anderson SJ, Burr DC. Spatial summation properties of directionally selective mechanisms in human vision. *J Opt Soc Am A.* 1991;8:1330-1339.
60. Adelson EH, Bergen JR. Spatiotemporal energy models for the perception of motion. *J Opt Soc Am A.* 1985;2:284-299.
61. Harwerth RS, Carter-Dawson L, Smith EL 3rd, Barnes G, Holt WF, Crawford ML. Neural losses correlated with visual losses in clinical perimetry. *Invest Ophthalmol Vis Sci.* 2004;45:3152-3160.
62. Garway-Heath DF, Caprioli J, Fitzke FW, Hitchings RA. Scaling the hill of vision: the physiological relationship between light sensitivity and ganglion cell numbers. *Invest Ophthalmol Vis Sci.* 2000;41:1774-1782.
63. Schein SJ, de Monasterio FM. Mapping of retinal and geniculate neurons onto striate cortex of macaque. *J Neurosci.* 1987;7:996-1009.